Journal of Pharmaceutical Sciences xxx (2020) 1-10

Contents lists available at ScienceDirect

Journal of Pharmaceutical Sciences

journal homepage: www.jpharmsci.org

Pharmaceutics, Drug Delivery and Pharmaceutical Technology

Molecular Dynamics Simulations Reveal Membrane Interactions for Poorly Water-Soluble Drugs: Impact of Bile Solubilization and Drug Aggregation

Aleksei Kabedev [a, c], Shakhawath Hossain [a, c], Madlen Hubert [a], Per Larsson [a, b], Christel A.S. Bergström [a, b, *]

[a] Department of Pharmacy, Uppsala University, Husargatan 3, 751 23 Uppsala, Sweden
[b] The Swedish Drug Delivery Center (SweDeliver), Uppsala University, Husargatan 3, 751 23 Uppsala, Sweden

ARTICLE INFO

Article history:
Received 14 August 2020
Revised 14 October 2020
Accepted 28 October 2020

Keywords:
Molecular dynamics
Intestinal fluid
Bile
Drug-membrane interactions
Amorphous aggregates
Micelle-membrane interaction

ABSTRACT

Molecular transport mechanisms of poorly soluble hydrophobic drug compounds to lipid membranes were investigated using molecular dynamics (MD) simulations. The model compound danazol was used to investigate the mechanism(s) by which bile micelles delivered it to the membrane. The interactions between lipid membrane and pure drug aggregates—in the form of amorphous aggregates and nanocrystals—were also studied. Our simulations indicate that bile micelles formed in the intestinal fluid may facilitate danazol incorporation into cellular membranes through two different mechanisms. The micelle may be acting as: i) a shuttle that presents the danazol directly to the membrane or ii) an elevator that moves the solubilized danazol with it as the colloidal structure itself becomes incorporated and solubilized within the membrane. The elevator hypothesis was supported by complementary lipid monolayer adsorption experiments. In these experiments, colloidal structures formed with simulated intestinal fluid were observed to rapidly incorporate into the monolayer. Simulations of membrane interaction with drug aggregates showed that both the amorphous aggregates and crystalline nanostructures incorporated into the membrane. However, the amorphous aggregates solubilized more quickly than the nanocrystals into the membrane, thereby improving the danazol absorption.

Introduction

Oral drug delivery is the most convenient and desirable route of drug administration for the treatment and prevention of many diseases. However, due to their poor aqueous solubility, absorption through the intestinal epithelium remains a challenge for many new oral drug candidates.[1-3] In the gastrointestinal tract (GIT), poorly soluble lipophilic drug molecules tend to form aggregates that can exist in amorphous or crystalline forms. In the GIT, lipophilic drug molecules also interact with naturally available colloidal structures and/or mixed micelles in the intestinal fluid, typically composed of bile salts and phospholipids.[3-5] During the interaction with the intestinal fluid, such molecules can be solubilized and become incorporated into the intestinal colloidal structures.[3] In these instances, the colloidal structures themselves bring the solubilized drug compounds closer to the absorption site. Previous studies show that solubilization of lipophilic or hydrophobic drug molecules into mixed micelles composed of bile salts and phospholipids can enhance the epithelial transport of hydrophobic compounds through transcellular routes.[6-10] Thus, drug molecules can approach the cell membrane as a free monomer or a small amorphous aggregate (Fig. 1a), in its crystalline form (Fig. 1b), or as a part of a colloidal structure (Fig. 1c and d). However, the molecular interaction pattern between these colloidal structures loaded with hydrophobic drug compounds and the intestinal membrane is poorly understood.

Danazol is a synthetic steroid with low oral bioavailability and water solubility. The crystal structure of danazol is shown in Supplementary Fig. 1. In model intestinal fluids, its solubility increases linearly with the concentration of most prominent intestinal components, bile salts and phospholipids.[11,12] The flux of danazol through the surface of the cell membrane can therefore be highly affected by these intestinal components. The clinical impact

* Corresponding author.
E-mail address: Christel.Bergstrom@farmaci.uu.se (C.A.S. Bergström).
[c] Equal contribution.

https://doi.org/10.1016/j.xphs.2020.10.061

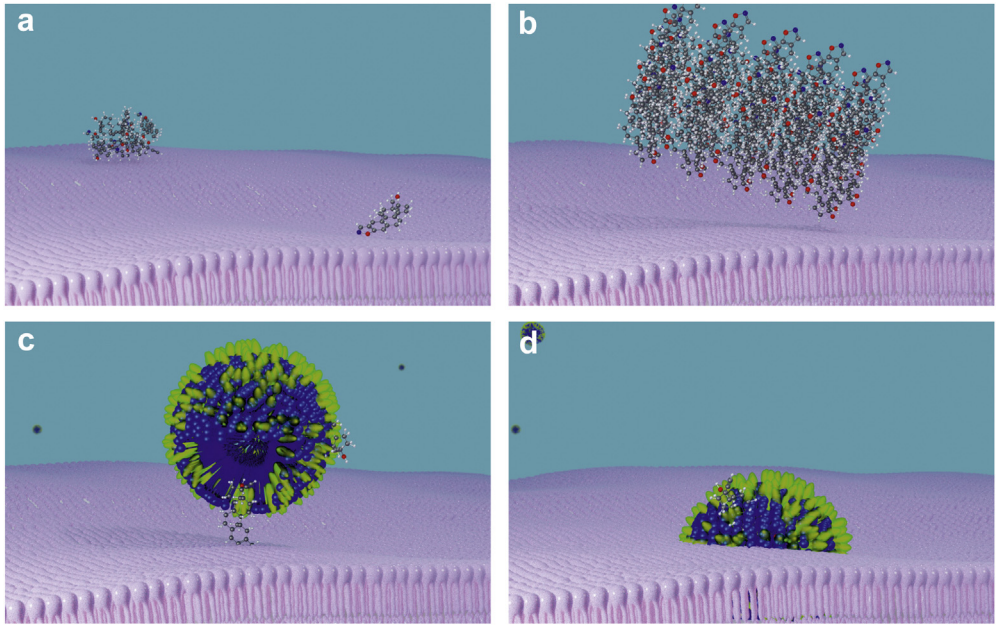

Fig. 1. Four scenarios of danazol incorporation into the cell membrane considered in the study: (a) as a free monomer or a small amorphous aggregate, (b) as a nanocrystal, (c) shuttled at the interface of the bile micelle and (d) fused as a part of a micelle.

of solubilizing danazol in bile colloidal structures has been reported, and an increased peak concentration and area-under-the-curve (AUC) was observed for danazol solubilized in the fed state as compared to the fasted state fluids.[13] Note that, due to higher bile secretion the presence of lipid content is higher in the fed state, and danazol is known to favor lipids.[14,15] The increased plasma concentration and AUC, in part, are indications of the impact of bile on danazol bioavailability.

Various experimental studies have investigated the drug-membrane or micelle-membrane interaction.[16-21] However, experimental studies most often can determine only macroscopic properties like drug permeability, rate of diffusion, or changes in the membrane such as surface area and thickness.[16,17] Molecular dynamics (MD) simulations are an alternative to experimental methods.[22,23] MD simulations can show molecular level details of membrane permeation of drug compounds,[18,24] structural changes of the lipid membranes during the drug permeation process,[19] aggregation behavior of intestinal fluid components,[25-27] and their interaction with drug components.[26,28] The all-atom (AA) MD simulation—in which each atom is represented individually—is more accurate, but computationally expensive and typically only used for shorter simulations of up to several microseconds and smaller systems length-wise. One approach for performing longer simulations and also making use of larger boxes during simulation is the coarse-grained (CG) methodology.[29,30] Although CG lacks the precision of the AA model by representing 3–4 heavy atoms with one bead, the upside is that it allows longer simulations to be run.

The aim of the present study was to investigate the molecular mechanism(s) by which a poorly water-soluble drug may be delivered and incorporated into the membrane. Danazol was used as the model compound and MD simulations were used to evaluate its interactions with intestinal membrane as a free monomer and an amorphous aggregate (Fig. 1a). Incorporation and solubilization into the lipid membrane were investigated for the monomers and aggregates, as well as nanocrystals of danazol (Fig. 1b). Finally, we investigated how a mixed micelle loaded with danazol interacted with the membrane and the possible transport mechanisms of the drug (Fig. 1c and d). Both AA- and CG MD simulations were run to evaluate the consistency between the methods and to obtain an improved molecular understanding of the drug-membrane interaction(s). In order to validate our computational observations, experimental measurements of colloidal size distribution and membrane adsorption were performed.

Experimental Section

All-Atom Molecular Dynamics (AA-MD)

All-atom simulations were performed with Gromacs 2018,[31] using the generalized amber force field (GAFF)[32,33] and Slipids force field.[34,35] To represent the intestinal bile components, sodium taurocholate (NaTC) and 1,2-dilinoleoyl-*sn*-glycero-3-phosphatidylcholine (DLiPC) were used. 1-palmitoyl-2-oleoyl-*sn*-glycero-3-phosphatidylcholine (POPC) was selected as the model lipid to represent lipid bilayer since phosphatidylcholine is a common phospholipid found in the plasma membrane of intestinal epithelial cells.[36] Topologies of danazol, DLiPC and NaTC molecules were produced via Stage software.[37] The electrostatic potentials were derived with PyRed server.[38] POPC membrane was taken from the Slipids force field webpage.[34] Simulations were run at 37 °C, with isotropic (without membrane), or with semi-isotropic pressure coupling, at 1 bar and compressibility of 4.5e-5. Nose-Hoover thermostat[39,40] and Parrinello-Rahman barostat[41] were applied for the production simulations.

Initial configurations of micelles were formed from randomly distributed NaTC and DLiPC molecules in water. After energy minimization and system equilibration, the production runs were performed (at least 10 ns) to obtain the micellular structures. A periodic boundary condition in all three box directions was applied in the simulations.

The potential of mean force (PMF) profiles were calculated using Umbrella Sampling (US) simulations.[42] Four different US simulations were performed in which the danazol molecule was pulled: i) from the danazol cluster to the water phase, ii) from the micelle to the water phase, iii) from the membrane center to the water phase, and iv) from the micelle to the membrane center (or in the opposite

direction) after placing the micelle adjacent to the membrane surface (see Supplementary Fig. 2).

In the US simulations, a series of configurations was generated along the reaction coordinate for each case described above. We generated a number of configurations separated at a distance of 0.1 nm along the reaction coordinate which served as the starting point for the US simulation. Each starting configuration was then energy minimized, equilibrated for 2 ns, followed by a production run for 20 ns. To extract the PMF along the reaction coordinate from the US simulations, the weighted histogram analysis method (WHAM) implemented in Gromacs as gmx wham utility was used.[43] For micellular structures, the Jacobian correction was made according to Equation (1).[44,45]

$$U(x) = U_0(x) + 2\, k_B T \ln(x) \quad (1)$$

where U denotes free energy or potential of mean force, k_B is the Boltzmann constant, T is the temperature in Kelvin and x is the distance along the reaction coordinate. Pulling force constant was gradually increased from the initial 3000 to 20,000 where needed, in order to fix the molecule at each bin across the whole range of x values.

For the first category of the US simulations (Supplementary Fig. 2a), 10 danazol molecules were initially randomly placed in the simulation box with water. Once the drug molecules underwent self-assembly and the aggregate was stable, a single danazol molecule was pulled out of the aggregate. The second group of the US simulations explored the effect of solubilization. One danazol molecule was equilibrated in the system with a mixed micelle until the molecule was solubilized into the micelle. The molecules of the mixed micelle were then fixed with a flat-bottom potential at two opposite ends (most distant heavy atoms of each molecule) and the danazol molecule was gradually pulled out of the mixed micelle (Supplementary Fig. 2b).

Danazol incorporation into the cell membrane was explored next. Danazol was initially pulled to the center of the POPC membrane and fixed there, until the water molecules following it towards the membrane (an effect of solvent drag) were pushed out by lipids. After equilibration, danazol was pulled out to the bulk and sampled with the US technique (Supplementary Fig. 2c).

The final category of US simulations explored direct danazol transfer between the bile micelle and the POPC membrane. The micelle with solubilized danazol was rotated to place the danazol molecule as close to the membrane as possible. Thereafter the micelle was pulled to the surface of the membrane which positioned the danazol at the interface between the POPC and NaTC-DLiPC micelle. The danazol molecule was then pulled along the normal direction from the membrane to the center of the bilayer. If water molecules followed the drug, they were removed from the membrane layer and the terminal heavy atoms of the DLiPC and NaTC molecules were fixed with flat-bottom potentials. After additional equilibration, the molecule was pulled back from the POPC membrane to the center of the micelle (Supplementary Fig. 2d). All simulations were repeated three times.

Amorphous aggregates of danazol formed in unbiased MD simulations were compared with the nanocrystal form by a radial distribution function (RDF). The calculations were performed with the gromacs function 'gmx rdf' on the nitrogen atoms. Collinearity of the drug molecules was evaluated with an order parameter. For that purpose, the coordinates of the opposite ends of the danazol molecules were used to define vectors. The variability of the angles was then measured with respect to the average direction of all drug molecules. The calculation was done with the in-house written script according to Equation (2).

$$S = \tfrac{1}{2}\left(3 < cos^2\theta > -1\right) \quad (2)$$

where θ is the angle between the vector of each drug molecule and the average direction of all drug molecules, and S is the order parameter.

Coarse-Grained Molecular Dynamics (CG-MD)

The CG-MD simulations were performed using the Martini force field for systems consisting of danazol, different bile components, and lipid membrane.[46,47] To develop the CG danazol model, AA-simulation with a single danazol molecule was performed using the amber force field as described in the previous section.[32,33] The all-atom danazol simulation was then used as reference data to obtain the Martini CG topology following the parameterization of new molecules described in the Martini website.[48] CG parameterization of sodium taurocholate was based on Martini cholesterol topology as described and validated in Clulow et al.[25] The CG topologies of phospolipids (POPC and DLiPC) are available at the Martini website.[47]

The POPC membrane was generated using the method Insane developed by Wassenaar et al.[49] The resulting bilayer from Insane was then equilibrated, resulting in a thickness of 4.05 nm and area per lipid of 0.65 nm^2 at 37 °C. These values are close to the experimentally measured ones for POPC membrane, which are 3.91 nm and 0.64 nm^2 at 30 °C, respectively, according to Kučerka et al.[50] The simulations were performed with the Gromacs 2018 software with semi-isotropic pressure coupling due to presence of lipid membrane in the system.[31] Each system was energy minimized using the steepest descent algorithm. This was followed by four short equilibration runs (50,000 steps) with time steps of 1, 2, 5, and 20 fs, before the final production run. A periodic boundary condition was applied for all simulations.

To perform the simulation with a danazol nanocrystal, the positions of the danazol atoms in crystalline structure were taken from the Cambridge Crystallographic Data Centre (CCDC), database identifier YAPZEU01.[51] The pattern was then used to construct three nanocrystals (8, 48 and 96 molecules) in Avogadro software.[52] During the CG simulation with the nanocrystal, the danazol molecules in the nanocrystal were restrained with a distance restraint matrix using the 'disre' option implemented in Gromacs as gmx genrestr utility.[31] The distance restraint matrix prevented deformation of the size and shape of the nanocrystals and kept the danazol molecules from leaving the nanocrystals during the simulation. These restrictions kept the nanocrystals from solubilizing during the simulation. Note that the simulation time-scale (in the range of μs) in this study was not large enough to capture nanocrystal solubilization, which is typically minutes for poorly water-soluble compounds.[53,54] Also, due to the use of the distance restraint matrix, a time step value of 10 fs was used in the simulations with nanocrystals. However, all the other CG simulations used a 30-fs time step.

All simulations were performed at 37 °C. CG-MD was also used for the US simulation, with the same working process as for the AA-MD simulations. The detailed system dimensions, simulation times, and components used in AA- and CG-simulations are in Supplementary Tables 1 and 2.

Preparation of Biorelevant Media for Experimental Measurements

A commercially available fasted state simulated intestinal fluid (FaSSIF) powder and an in-house mixture of a bile salt and phospholipid were used to study the interactions of micelles with

the POPC membrane. FaSSIF is commonly used and easily reproducible, while the mixture of bile salt/phospholipid better matches the computational setup. FaSSIF buffer (pH 6.5) was used to prepare the biorelevant media and comprised 10.5 mM sodium hydroxide, 28.7 mM sodium phosphate monobasic anhydrous and 105.9 mM sodium chloride, prepared in Milli-Q water (MQ water, Milli-Q Advantage A10, resistivity of 18.2 MΩ cm, Merck Millipore, Billerica, MA, USA). A 100-fold stock solution of FaSSIF V1 (Biorelevant.com Ltd, London, UK) was prepared from powder according to manufacturer's instructions, containing taurocholate and phospholipids at a 4:1 M ratio. To produce the in-house medium, 1,2-dioleoyl-*sn*-glycero-3-phosphocholine (DOPC Avanti Polar Lipids Inc., Alabaster, AL, US) was used as a highly purified phospholipid. The required amount of DOPC was dissolved in chloroform (purity 99.0–99.4%, VWR, Stockholm, Sweden) and a thin lipid film was generated using a stream of nitrogen gas. An appropriate amount of sodium taurodeoxycholate hydrate (NaTC, Sigma Aldrich, St. Louis, MO, US) was added to the vial and both components were dissolved in FaSSIF buffer to achieve a final concentration of 300 mM NaTC and 75 mM DOPC (4:1 M ratio). The solution was sonicated (Transsonic T 310, Elma, Singen, Germany) for 2 h and frequently vortexed during sonication.

Dynamic Light Scattering (DLS) Measurements

DLS measurements were performed on a Malvern Zetasizer Nano-S (Malvern Instruments, Worcestershire, UK) to determine the size distribution of FaSSIF V1 and the in-house preparation. Each of the stock solutions was diluted 1:100 with FaSSIF buffer and samples were measured in UV-transparent disposable cuvettes (Sarstedt, Nümbrecht, DE) at 25 °C. Peak mean sizes are reported from intensity distribution. The Nano DTS Software 5.0 was used for acquisition and analysis of the data. All measurements were performed in triplicates.

Lipid Monolayer Adsorption Experiments

Lipid monolayer experiments were performed in a custom-built round trough with a volume capacity of 10 mL (Kibron Inc., Helsinki, Finland) according to a previously reported method.[55] The trough was covered to prevent temperature and humidity loss. Before each experiment, the trough was thoroughly cleaned with chloroform and washed with MQ water. A microbalance equipped with a DyneProbe (Kibron) consisting of metal alloy was used to measure the surface pressure (π) and calibrated before each experiment. A 1 mM stock solution of 1-palmitoyl-2-oleoyl-*sn*-glycero-3-phosphocholine (POPC, Avanti Polar Lipids, Inc., Alabama, USA) was prepared in chloroform. The POPC solution was deposited onto the surface of the subphase (FaSSIF buffer) using a Hamilton microsyringe to obtain the required initial surface pressure π_0 (20 mN m^{-1}). After 10 min of solvent evaporation a stable monolayer was formed, and each of the two variants of biorelevant media were injected underneath the monolayer into the subphase. A volume of 100 μL of each stock solution was injected to achieve adequate concentration of FaSSIF V1 (3 mM taurocholate and 0.75 mM phospholipids) and of the in-house preparation (3 mM NaTC and 0.75 mM DOPC). All experiments were carried out under constant stirring at 25 °C and the adsorption isotherm of the two experiments was obtained. Data were recorded using FilmWareX 4.0 and analyzed with Prism 5.0 (Graph-Pad, San Diego, CA, US).

Results and Discussion

Interaction of Free Drug Molecules and Small Amorphous Aggregates with Membranes

The interaction and solubilization of free drug molecules and amorphous aggregates with lipid bilayers were investigated by unrestrained AA- and CG-MD simulations. First, one danazol molecule was randomly placed near the membrane to represent an infinite dilution of danazol. The simulations were repeated ten times and, in all cases, resulted in the incorporation of the danazol molecule into the membrane. The average time for danazol incorporation into the membrane was in the order of 100 ns and 40 ns for AA- and CG-methods, respectively. In other words, reducing the resolution of the method still captured the same event but reduced the time needed by 2.5-fold. Once the danazol reached the surface of the POPC membrane, the permeation typically occurred within 10 ns. An example of the insertion process of danazol is depicted in Fig. 2. After inserting into the membrane, danazol molecules remained inside the membrane for the rest of the simulation, buried relatively deeply inside the bilayer structure.

Free drug molecules near the membrane at a concentration higher than the aqueous solubility of the drug can lead to precipitation and the formation of small aggregates. These aggregates can be amorphous or nanocrystalline. Danazol quickly forms nanocrystals in pure water,[56] but polymers and naturally occurring components in the intestinal fluid may result in amorphous aggregates.[57] To investigate the interaction of amorphous aggregates and lipid bilayer, we performed 2-μs unrestrained simulations using both AA- and CG-MD methods. A small amorphous aggregate with 10 danazol molecules was first generated and placed near the membrane. During both the AA- and CG-simulations, this aggregate was incorporated into the membrane and thereafter solubilized by the membrane, i.e., the amorphous aggregate dissolves once incorporated into the phospholipid bilayer (Fig. 3).

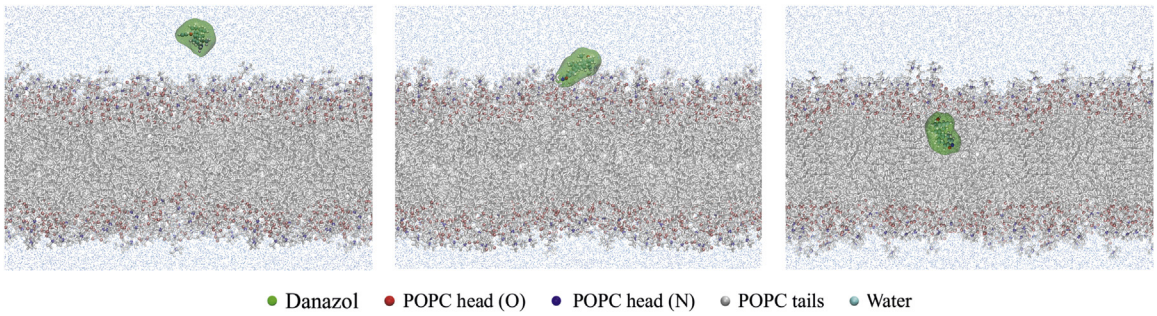

Fig. 2. Incorporation of danazol into the POPC membrane at three stages: in bulk, at the surface of the membrane, and incorporated into the bilayer. Representative snapshots were taken from all-atom molecular dynamics simulation.

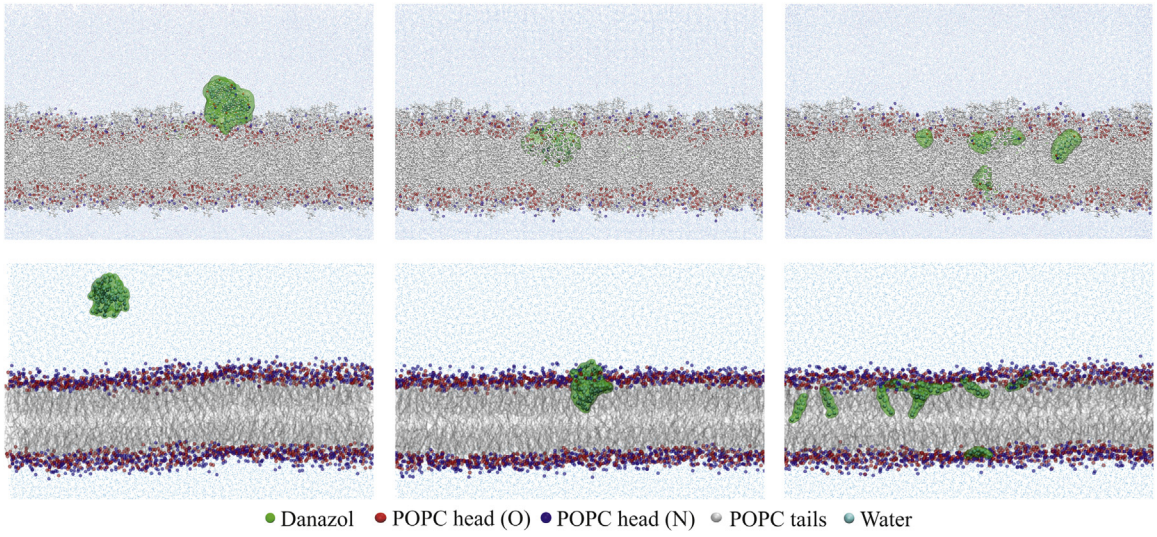

Fig. 3. Interaction of amorphous danazol aggregate and lipid membrane. Representative simulation snapshots exhibiting amorphous danazol aggregate incorporation and solubilization inside the lipid membrane: all-atom simulation (upper panel; snapshots representing 0, 600 and 2000 ns) and coarse-grained simulation (lower panel; snapshots representing 0, 900 and 2000 ns).

Interestingly, the danazol molecules did not dissociate from the aggregate to permeate the membrane. Note that, for amorphous aggregate, danazol molecules were not constrained to be together and the molecules were allowed to dissociate from the aggregate. In all simulations, the insertion of the danazol only occurred for the whole cluster. That might be because all danazol molecules are similarly attracted towards the inner layer of the membrane. As they are being pulled together during the US simulation, penetration is more likely to take place where the entire aggregate can be sterically accommodated inside the membrane. This was observed in both the AA and CG simulations, where the separation of the molecules from the cluster occurred only within the membrane. In the AA simulations, the aggregate was incorporated into the membrane at around 600 ns after contact with the membrane. After the membrane incorporation, the amorphous aggregate broke up within a microsecond and the molecules were dissolved in the membrane. The separate free danazol molecules remained inside the membrane for the rest of the simulation. Inside the membrane, the danazol molecules localized slightly below the lipid headgroup region. As indicated by the mass density profiles, the positions of the danazol molecules are found between the peaks of the lipid head groups of the two leaflets (Supplementary Fig. 3).

The CG-simulations showed a similar interaction of the amorphous aggregate with the lipid membrane. The amorphous aggregate incorporated into the membrane at around 900 ns and at around 1000 ns, the molecules from the aggregates were solubilized by the membrane. The solubilized danazol molecules remained inside the membrane and were located slightly below the lipid head groups also in the CG-MD simulations (Supplementary Fig. 3). Note that the membrane incorporation of the amorphous aggregate during the CG-simulations required longer (900 ns) than the AA-simulations (600 ns). This is mainly due to the fact that the volume of the CG-simulation box was about 10 times higher than the box used in AA-simulations.

We then performed detailed analysis of the danazol amorphous aggregate formed in the AA simulations and compared it with its crystalline counterpart. The trajectory files from MD simulations were analyzed for aggregates of 5, 10 and 100 molecules of danazol in water; for the crystalline form of danazol, the Cambridge Structural Database was used as reference. We observed that the hydrophobic carbon rings of danazol molecules have high affinity to themselves, whereas the oxygen and nitrogen atoms prefer interactions with like atoms or with water molecules. This affinity leads to an alignment of the molecules, as can be seen in Fig. 4. Such

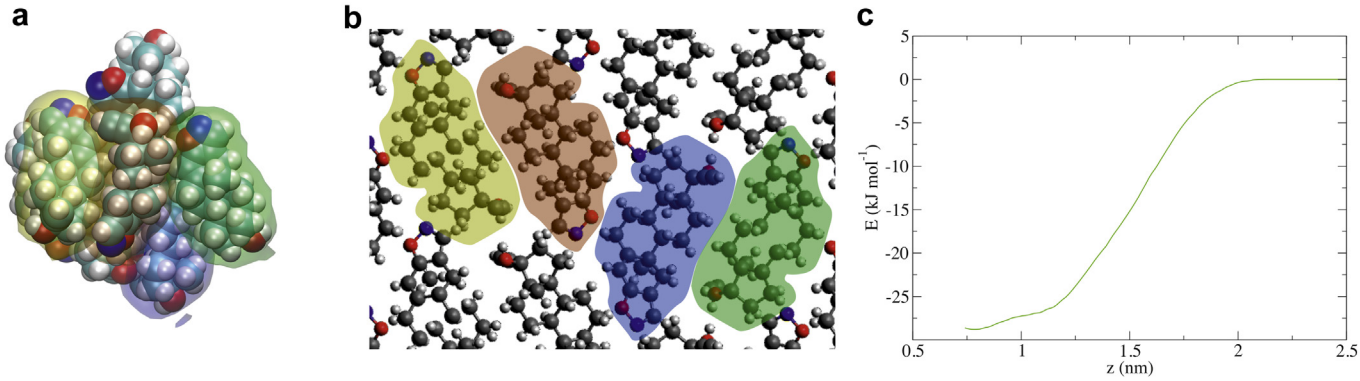

Fig. 4. Analysis of danazol molecules presence in amorphous aggregate or nanocrystal. (a) Snapshot of a 10 API molecules cluster, as observed from AA simulations (water is omitted); (b) a crystalline organization of the molecules in solid danazol; (c) free energy profile of the danazol molecule pulled away from the cluster of 10 APIs.

organization of the molecules can be observed over a short time for smaller amorphous aggregates of molecules (5 and 10 drug molecules). However, for a bigger cluster of 100 APIs, many molecules are stuck in local energy minima and do not reorganize as a crystal within a 200-ns simulation. We assume that head-to-tail or head-to-head organization obtained for the smaller aggregates indicates a tendency to crystallization. Nevertheless, the actual intermolecular interactions are being overly smoothened to observe realistic crystallization in MD simulations. We propose that crystallization could take longer times, specifically for relatively large clusters of molecules.

Radial distribution function (RDF) was used to analyze the distances between the oxygen and nitrogen atoms of all danazol molecules. Even for smaller aggregates, where a good alignment was seen in the MD simulation, the RDF profiles of danazol amorphous aggregates and nanocrystals differed significantly. This difference originates from the discrete form of the RDF for nanocrystals, and from the closer packing of the molecules in the amorphous aggregates. Another tool used to quantify the organization of the danazol was the order parameter - *S*. It represents the average degree of collinearity between each individual molecule from the cluster and the average direction of all of them. The value of *S* spans from −0.5 to 1.5, where −0.5 indicates complete absence of order in the orientation of the molecules, and 1.5 indicates absolute collinearity of the molecules in the aggregate (see Eq. (2)). We observed that even the molecules of a perfectly organized danazol nanocrystal did not have a high order value, as several subgroups of collinear molecules are presented, that in average give a low value of order parameter. *S* was calculated to be 0.06 for the danazol nanocrystal, 0 for the amorphous aggregate of 100 molecules, and 0.02 for the aggregate with 10 molecules. Thus, the values are relatively close to each other. MD simulations are not able to represent crystallization at such level of detail, but based on indirect indications, we conclude that the drug molecules would quite likely crystallize rapidly, once surrounded by water.

We then performed US simulations to evaluate the energy associated with the removal of a danazol molecule from an amorphous aggregate consisting of 10 danazol molecules (as in Fig. 4a). The danazol molecule preferred to be in the aggregate rather than in the bulk water phase (Fig. 4c). There was no difference in energy cost for danazol molecules pulled from the aggregate surface or the aggregate center to the bulk. It was ~28 kJ/mol in both AA and CG simulations.

These results indicate that, in addition to the free danazol monomers, small amorphous danazol aggregates can also incorporate into the membrane. After incorporation, solubilization of the aggregate occurs fairly quickly and the danazol molecules diffuse within the lipid bilayer. While MD simulations cannot confirm a rapid crystallization of the danazol molecules, it seems likely when the molecules are surrounded by water. This is in line with literature reports of rapid crystalline precipitation of danazol when at concentrations higher than solubility limit.[58]

Incorporation of Danazol Nanocrystals in Cell Membrane

To investigate the incorporation of danazol nanocrystals in the lipid membrane, an approach similar to the one described for the amorphous aggregate was adopted. The danazol nanocrystal was placed near the lipid membrane and CG-MD simulations were run for 2 μs. Three differently sized crystals of 8, 48 and 96 danazol molecules were used in the simulations. Details of the crystalline dimensions are shown in Supplementary Table 3. Note that the crystalline structures were modelled in such a way that molecules could not detach from the crystal and its size and shape could not be deformed (see methods section Coarse-Grained Molecular Dynamics (CG-MD)).

Similar to the amorphous aggregates, all three nanocrystals incorporated into the membrane within 200 ns of the simulation and remained there for the rest of the simulation (2 μs). Note that, membrane incorporation of hydrophobic nanoparticle with various sizes and shapes were also observed in both experimental and computational studies.[59,60] The initial and final snapshot of the simulation for each nanocrystal size is presented in Supplementary Fig. 4. The interaction of the nanocrystals with the membrane differed depending on crystal size. The smallest nanocrystal (8 molecules) inserted into the membrane and mostly remained in the upper leaflet of the membrane. This is indicated by the mass density profiles where the peak of the lipid headgroup for the upper leaflet is at 5.77 nm and the density of the danazol cluster spans between 3.35 and 5.50 nm (Supplementary Fig. 5). Note that the center of the membrane is estimated to be at 3.75 nm. Both the medium-sized (48 molecules) and largest nanocrystal (96 molecules) immersed themselves into the membrane and spanned both leaflets. The largest nanocrystal also significantly affected the membrane properties and displaced some of the lipid molecules from the membrane. The loose lipid molecules then attached to the surface of the nanocrystal as shown in Supplementary Fig. 4c.

The simulation results here suggest that nanocrystals of the hydrophobic drug danazol preferred to interact with the lipid membrane rather than the water phase. Like the amorphous aggregates, the nanocrystals became incorporated into the membrane. Upon membrane incorporation, the amorphous aggregates were quickly solubilized within the lipid bilayer. Note that, due to the lack of proper drug-drug interaction parameter values within the nanocrystal when incorporated into the membrane as well as the (still) limited time scale of the simulations, the solubilization mechanism of the nanocrystals in the membrane was not possible to investigate using MD. In our simulations, a restraint to keep the drug molecules within the nanocrystal was used. However, the literature seems to offer a consensus that the nanocrystals can often form a strong crystal lattice which show a limited capacity to dissociate from solid form. Therefore, the observations in this section i.e. the lack of nanocrystals dissociation capacity in the membrane and changing membrane properties might be relevant for such compounds at smaller time scale. Indeed, this may be one reason why amorphous solid formulation achieve better permeability through the intestinal membrane than crystalline formulations.[61,62]

Interaction of Membrane and Danazol Loaded FaSSIF Micelle

In the intestine, lipophilic drug molecules can be solubilized by the intestinal colloidal structures, and once near the membrane, those colloidal structures interact with the membrane. To investigate how such drug-loaded intestinal micelles interact with the lipid membrane, the simulations used a small micelle typically observed with FaSSIF components. These micelles were loaded with danazol and the potential of mean force was calculated from US simulation with the AA- and CG-methods. In these simulations, danazol was pulled:

1. from the micelle to the water phase,
2. from the membrane center to the water phase, and
3. from the micelle to the membrane center after placing the micelle adjacent to the membrane surface.

The PMF profiles shown in Fig. 5 clearly indicate that the hydrophobic danazol molecule prefers to stay in association with the micelle or inside the membrane (Supplementary Table 4). In the AA

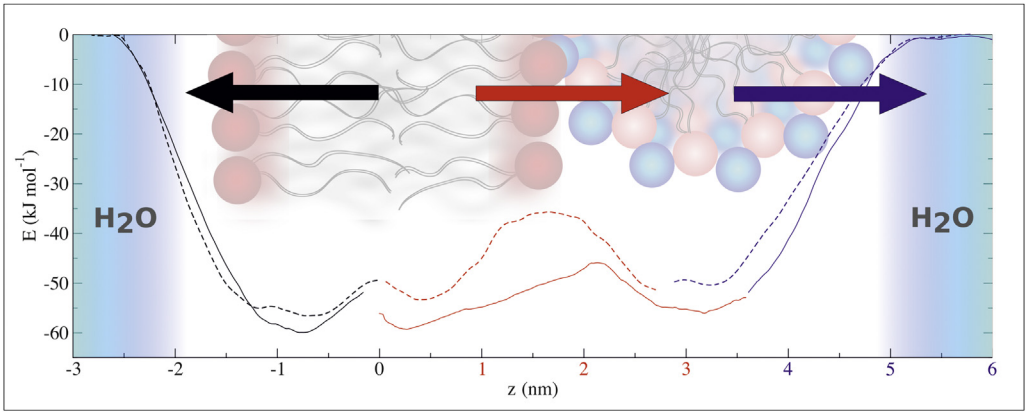

Fig. 5. Combined free energy profiles graphs for danazol pulled from the micelle to bulk (blue lines), from the membrane to bulk (black line) and from the membrane to the micelle (red line). Solid lines represent results from AA simulations, dashed lines – for CG. The origin along the z-axis is taken at the center of the membrane. In the micelles the molecules were pulled not to the center, but to the potential well, where the danazol molecules are in the lowest free energy state.

simulation of danazol pulled from micelle and membrane to water, the energy minima were found to be near the micelle shell region and slightly above the membrane center. The free energy difference, ΔG, required to move the danazol molecule from the micelle was 54 kJ/mol and 60 kJ/mol for membrane center to the water phase. However, when the micelle was placed adjacent to the membrane surface, the ΔG required to move the danazol molecule from the micelle to membrane center was only 14 kJ/mol. This is 3.8 and 4.3 times lower than the ΔG for moving the danazol molecule from the micelle and membrane center to the water phase, respectively. From the depths of the wells in the free energy profiles, one can see that the lower energy state would be reached if the danazol molecule were placed in the POPC layer instead of in the micelle. This suggests that during the interaction of intestinal micelles loaded with hydrophobic drug molecules, the drug molecule can be passively transported from the colloidal structure to the membrane if thermal fluctuations (or other factors) cause an excess energy equal or higher than 14 kJ/mol. As described in section Interaction Of Free Drug Molecules And Small Amorphous Aggregates With Membranes, the free energy difference to pull a single danazol molecule from a cluster of 10 molecules is significantly lower (29 kJ/mol) than the corresponding values for micelle-to-water and membrane-to-water transitions. This further supports the concept that a danazol molecules in the form of amorphous aggregate will likely incorporate into the membrane or micelle after being in contact for a certain time.

Similar results were obtained using the CG simulations. The ΔG required to move the danazol molecule the micelle and membrane center to the water phase were 51 and 57 kJ/mol, respectively. In contrast, only 18 kJ/mol was needed to move the danazol molecule from the micelle to membrane center. Again, the two different simulation methodologies were in good qualitative agreement. ΔG values obtained from both AA- and CG-simulations for different systems are summarized in Supplementary Table 4. As predicted from the experimentally observed logP value danazol should be most attracted to the cell membrane, which is confirmed by our simulations here. The lower energy barrier required to move a danazol molecule from a bile micelle to the membrane center observed in both methods suggests that the micelle may act as a shuttle to deliver danazol to the membrane.

We then performed unrestrained simulations in which a micelle containing FaSSIF and danazol was placed in the water phase above the POPC membrane in a simulation box. Simulations of 2 μs were performed with both the AA- and CG-methods. In the AA simulation, one taurocholate detached from the micelle and inserted into the membrane, whereas the rest of the micelle remained in the colloidal form. However, in the CG-simulations, the micelle acted as an elevator, fused at the membrane insertion site taking the solubilized danazol with it when merging with the bilayer. Upon fusion, the whole micelle becomes solubilized into the membrane. The snapshots of the initial and final state of the simulations are shown in Fig. 6.

In the AA simulations, the micelle released a taurocholate molecule after a long contact time with the micelle. Based on this, it is expected that, with time, the micelle would fuse entirely into the membrane. This would produce a flux of molecules from the micelle to the membrane. Similar to the simulations with 10 danazol clusters (section Interaction Of Free Drug Molecules And Small Amorphous Aggregates With Membranes), this leads to a higher probability for the drug molecules to be transported towards the POPC membrane. Supplementary Fig. 6 shows the free energy profiles of the bile salt and phospholipid molecules pulled from the center of the POPC membrane. The energy required to pull both the NaTC and the DLiPC molecules from the membrane is approximately equal to 100 kJ/mol. This indicates a good affinity between the micelle components and membrane lipids and supports the fusion observation.

Overall, both the unrestrained and restrained MD simulations indicate that intestinal micelles are capable of delivering drug molecules to the membrane via interaction with the membrane. The higher affinity of danazol components for the intestinal micelles also suggests that intestinal components can prevent the formation of danazol nanocrystals and hence, subsequently increase danazol absorption through the intestinal membrane.

Investigating the Interaction of Fasted Intestinal Fluids With Lipid Monolayers as Model Membranes

To complement the MD simulations, two different simulated fasted state intestinal fluids were assessed in their interaction with lipid monolayers. Both media were prepared using FaSSIF buffer. DLS measurements of FaSSIF V1 revealed a uniform particle size distribution with a mean diameter of approximately 75.1 nm (Table 1), in agreement with previously reported size distributions.[63] In contrast to the homogeneous FaSSIF V1, the in-house preparation was polydisperse, with two peak mean sizes at 267.2 nm and 6.8 nm corresponding to a relative mass composition of 70% and 30%, respectively. A diameter of 6.8 nm is reasonably close to the size of the micelles simulated with MD.

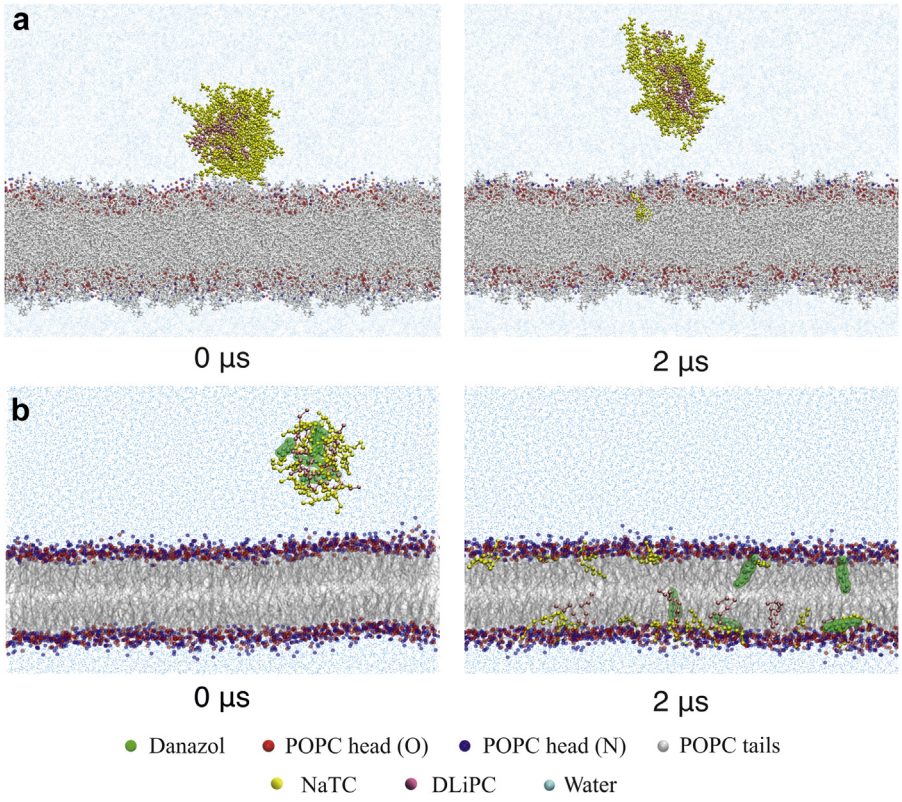

Fig. 6. Interaction of drug-loaded mixed micelle and lipid membrane. Snapshot of the simulations performed with (a) all-atom and (b) coarse-grained molecular dynamics methods at the initial and final time steps. In the all-atom simulation only one bile salt molecule detached from the micelle and incorporated into the membrane during the 2 μs. In CG the entire micelle got fused and distributed within the membrane during the same timeframe.

To further understand the interplay between the colloidal components within the simulated intestinal fluids and membranes in an experimental setting, their interactions were studied using lipid monolayers. These experiments were performed to support the hypothesis that micelles act as an elevator that moves the solubilized danazol with it as the colloidal structure itself becomes incorporated and solubilized within the membrane. Though vastly simplified, lipid monolayers provide a model of a half bilayer and can mimic essential physical and chemical properties of biological membranes. These films (i.e., monolayers) can be formed at the air/water interface of a Langmuir trough by spreading the lipids of interest. Parameters such as composition of the monolayer and the subphase (pH, ionic strength) as well as temperature can be varied in a controlled way.[64]

In our experiment, POPC was used to prepare lipid monolayers to closely resemble the conditions used for the MD simulations. The simulated intestinal fluid was then injected into the subphase, and the change in surface pressure ($\Delta\pi$) monitored over time (Fig. 7). Changes in surface pressure provide valuable information on whether colloidal structures, such as the micelles present in the biorelevant media, incorporate into the monolayer. For instance, when components incorporate into the lipid film, surface pressure increases, while a negative surface pressure suggests the loss of phospholipids from the interface into the subphase.[65] When FaSSIF V1 or the in-house medium was injected underneath a lipid monolayer, an instant and sharp increase in surface pressure was recorded ($\Delta\pi \approx 15$ mN m^{-1}). This indicates that the components found in both FaSSIF and the in-house medium adsorb to, and incorporate into, the POPC lipid monolayer. These experiments demonstrate the strong affinity of colloidal structures in both media for membranes and their ability to penetrate lipid layers. These results are in agreement with the CG-MD simulation, which suggests that mixed micelles composed of intestinal fluids will be incorporated and solubilized into the lipid membrane.

Table 1
Size Characterization by DLS of Biorelevant Media.

Simulated Intestinal Fluid	Peak	Diameter (nm)	Mass Composition (%)
FaSSIF V1	1	75.1 (±0.2)	100.0 (±0.0)
In-house preparation	1	267.2 (±8.5)	70.0 (±0.6)
	2	6.8 (±0.1)	30.0 (±0.6)

Data is shown as mean ± SD from the intensity distribution measurements ($n = 3$).

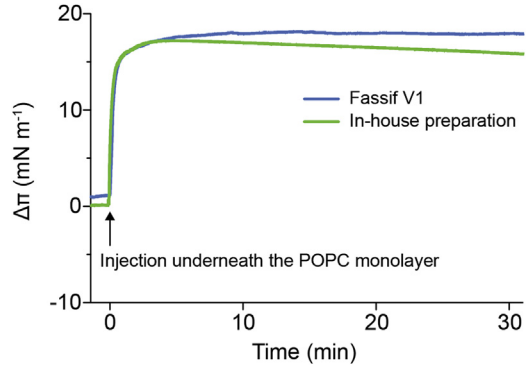

Fig. 7. Representative adsorption isotherms of biorelevant media to POPC monolayers. The samples were injected underneath the equilibrated film at time 0 min and the change in surface pressure ($\Delta\pi$) was monitored over time.

Conclusions

The transport mechanisms of danazol to lipid bilayers were investigated in depth by a series of computational simulations complemented with experimental studies. We found that bile micelles formed in the intestinal fluid may act as drug delivery shuttles and facilitate danazol incorporation into cellular membranes. This may occur through two different mechanisms. The micelle may shuttle the danazol directly to the membrane in which case the drug molecule does not need to pass via the aqueous phase to become absorbed. In the other mechanism, the micelle acts as an elevator, taking the solubilized danazol with it into the membrane as the colloidal structure becomes incorporated. The experimental studies confirmed the elevator hypothesis by finding that the colloidal structures of simulated intestinal fluid incorporated into the lipid bilayers rapidly and efficiently.

Danazol molecules that are not solubilized by the colloidal structures may precipitate if their concentration is higher than the aqueous solubility. In our computational simulations, both the amorphous aggregates and nanocrystals incorporated into the membrane. Once incorporated, the amorphous aggregates quickly dissolved in the membrane. For this type of aggregates, membrane solubilization may further facilitate absorption.

Supplementary Data

Supplementary data to this article is available.

Conflicts of Interest

The authors have no conflict of interest.

Acknowledgements

This study is part of an associated research project to the Swedish Drug Delivery Center (SweDeliver). The work was supported by the European Research Council (Grant 638965). The computations/data handling were enabled by resources provided by the Swedish National Infrastructure for Computing (SNIC) at the Uppsala Multidisciplinary Center for Advanced Computational Science (UPPMAX), the Center for High Performance Computing (PDC), and the High-Performance Computing Center North (HPC2N) partially funded by the Swedish Research Council through grant agreement no. 2018−05973. We also thank Prof. Richard Lundmark (Umeå University, Sweden) for access to the Langmuir trough.

Appendix A. Supplementary Data

Supplementary data to this article can be found online at https://doi.org/10.1016/j.xphs.2020.10.061.

References

1. Di L, Kerns E, Carter G. Drug-like property concepts in pharmaceutical design. *Curr Pharm Des*. 2009;15(19):2184-2194.
2. Homayun B, Lin X, Choi HJ. Challenges and recent progress in oral drug delivery systems for biopharmaceuticals. *Pharmaceutics*. 2019;11(3):129.
3. Boyd BJ, Bergström CAS, Vinarov Z, et al. Successful oral delivery of poorly water-soluble drugs both depends on the intraluminal behavior of drugs and of appropriate advanced drug delivery systems. *Eur J Pharm Sci*. 2019;137(June):104967.
4. Bergström CAS, Holm R, Jørgensen SA, et al. Early pharmaceutical profiling to predict oral drug absorption: current status and unmet needs. *Eur J Pharm Sci*. 2014;57(1):173-199.
5. Riethorst D, Mols R, Duchateau G, Tack J, Brouwers J, Augustijns P. Characterization of human duodenal fluids in fasted and fed state conditions. *J Pharm Sci*. 2016;105(2):673-681.
6. O'Reilly JR, Corrigan OI, O'Driscoll CM. The effect of simple micellar systems on the solubility and intestinal absorption of clofazimine (B663) in the anaesthetised rat. *Int J Pharm*. 1994;105(2):137-146.
7. Meaney CM, O'Driscoll CM. A comparison of the permeation enhancement potential of simple bile salt and mixed bile salt:fatty acid micellar systems using the CaCo-2 cell culture model. *Int J Pharm*. 2000;207(1-2):21-30.
8. Miyake M, Minami T, Hirota M, et al. Novel oral formulation safely improving intestinal absorption of poorly absorbable drugs: utilization of polyamines and bile acids. *J Control Release*. 2006;111(1-2):27-34.
9. Mukaizawa F, Taniguchi K, Miyake M, et al. Novel oral absorption system containing polyamines and bile salts enhances drug transport via both transcellular and paracellular pathways across Caco-2 cell monolayers. *Int J Pharm*. 2009;367(1-2):103-108.
10. Stojančević M, Pavlović N, Goločorbin-Kon S, Mikov M. Application of bile acids in drug formulation and delivery. *Front Life Sci*. 2013;7(3-4):112-122.
11. Pedersen BL, Müllertz A, Brøndsted H, Kristensen HG. A comparison of the solubility of danazol in human and simulated gastroiatestinal fluids. *Pharm Res (N Y)*. 2000;17(7):891-894.
12. Vertzoni M, Markopoulos C, Symillides M, Goumas C, Imanidis G, Reppas C. Luminal lipid phases after administration of a triglyceride solution of danazol in the fed state and their contribution to the flux of danazol across Caco-2 cell monolayers. *Mol Pharm*. 2012;9(5):1189-1198.
13. DANOCRINE® brand of DANAZOL CAPSULES, USP, U.S. Food and drug administration. https://www.accessdata.fda.gov/drugsatfda_docs/label/2011/017557s033s039s040s041s042lbl.pdf. 2013:1-9. http://www.accessdata.fda.gov/scripts/cder/iig/index.cfm.
14. Alskär LC, Porter CJH, Bergström CAS. Tools for early prediction of drug loading in lipid-based formulations. *Mol Pharm*. 2016;13(1):251-261.
15. Persson LC, Porter CJH, Charman WN, Bergström CAS. Computational prediction of drug solubility in lipid based formulation excipients. *Pharm Res (N Y)*. 2013;30(12):3225-3237.
16. Seddon AM, Casey D, Law RV, Gee A, Templer RH, Ces O. Drug interactions with lipid membranes. *Chem Soc Rev*. 2009;38(9):2509-2519.
17. Knobloch J, Suhendro DK, Zieleniecki JL, Shapter JG, Köper I. Membrane-drug interactions studied using model membrane systems. *Saudi J Biol Sci*. 2015;22(6):714-718.
18. Lopes D, Jakobtorweihen S, Nunes C, Sarmento B, Reis S. Shedding light on the puzzle of drug-membrane interactions: experimental techniques and molecular dynamics simulations. *Prog Lipid Res*. 2017;65:24-44.
19. Alves AC, Magarkar A, Horta M, et al. Influence of doxorubicin on model cell membrane properties: insights from in vitro and in silico studies. *Sci Rep*. 2017;7(1):1-11.
20. Treyer A, Mateus A, Wiśniewski JR, Boriss H, Matsson P, Artursson P. Intracellular drug bioavailability: effect of neutral lipids and phospholipids. *Mol Pharm*. 2018;15(6):2224-2233.
21. Khadka NK, Cheng X, Ho CS, Katsaras J, Pan J. Interactions of the anticancer drug tamoxifen with lipid membranes. *Biophys J*. 2015;108(10):2492-2501.
22. Haile JM. *Molecular Dynamics Simulation: Elementary Methods*. New York: Wiley; 1992.
23. Vlugt TJ, Van der Eerden JP, Dijkstra M, Smit B, Frenkel D. *Introduction to Molecular Simulation and Statistical Thermodynamics*. The Netherlands: First. Delft; 2009.
24. Yue Z, Li C, Voth GA, Swanson JMJ. Dynamic protonation dramatically affects the membrane permeability of drug-like molecules. *J Am Chem Soc*. 2019;141(34):13421-13433.
25. Clulow AJ, Parrow A, Hawley A, et al. Characterization of solubilizing nanoaggregates present in different versions of simulated intestinal fluid. *J Phys Chem B*. 2017;121(48):10869-10881.
26. Parrow A, Larsson P, Augustijns P, Bergström CAS. Molecular dynamics simulations on interindividual variability of intestinal fluids: impact on drug solubilization. *Mol Pharm*. 2020;17:3837-3844.
27. Vila Verde A, Frenkel D. Kinetics of formation of bile salt micelles from coarse-grained Langevin dynamics simulations. *Soft Matter*. 2016;12(23):5172-5179.
28. Holmboe M, Larsson P, Anwar J, Bergström CAS. Partitioning into colloidal structures of fasted state intestinal fluid studied by molecular dynamics simulations. *Langmuir*. 2016;32(48):12732-12740.
29. Levine BG, Lebard DN, Devane R, Shinoda W, Kohlmeyer A, Klein ML. Micellization studied by GPU-accelerated coarse-grained molecular dynamics. *J Chem Theor Comput*. 2011;7(12):4135-4145.
30. Hossain MS, Berg S, Bergström CAS, Larsson P. Aggregation behavior of medium chain fatty acids studied by coarse-grained molecular dynamics simulation. *AAPS PharmSciTech*. 2019;20(2):61.
31. Abraham MJ, Murtola T, Schulz R, et al. Gromacs: high performance molecular simulations through multi-level parallelism from laptops to supercomputers. *SoftwareX*. 2015;1−2:19-25.
32. Wang J, Wang W, Kollman PA, Case DA. Automatic atom type and bond type perception in molecular mechanical calculations. *J Mol Graph Model*. 2006;25(2):247-260.
33. Wang J, Wolf RM, Caldwell JW, Kollman PA, Case DA. Development and testing of a general Amber force field. *J Comput Chem*. 2004;25(9):1157-1174.
34. Jämbeck JPM, Lyubartsev AP. An extension and further validation of an all-atomistic force field for biological membranes. *J Chem Theor Comput*. 2012;8(8):2938-2948.

35. Jämbeck JPM, Lyubartsev AP. Derivation and systematic validation of a refined all-atom force field for phosphatidylcholine lipids. *J Phys Chem B*. 2012;116(10):3164-3179.
36. Koichi K, Michiya F, Makoto N. Lipid components of two different regions of an intestinal epithelial cell membrane of mouse. *Biochim Biophys Acta*. 1974;369(2):222-233.
37. Lundborg M, Lindahl E. Automatic GROMACS topology generation and comparisons of force fields for solvation free energy calculations. *J Phys Chem B*. 2015;119(3):810-823.
38. Vanquelef E, Simon S, Marquant G, et al. R.E.D. Server: a web service for deriving RESP and ESP charges and building force field libraries for new molecules and molecular fragments. *Nucleic Acids Res*. 2011;39(Suppl. 2):511-517.
39. Nosé S. A molecular dynamics method for simulations in the canonical ensemble. *Mol Phys An Int J Interface Between Chem Phys*. 1984;52:255-268.
40. Hoover WG. Canonical dynamics: equilibrium phase-space distributions. *Phys Rev A*. 1985;31:1695.
41. Parrinello M, Rahman A. Polymorphic transitions in single crystals: a new molecular dynamics method. *J Appl Phys*. 1981;52(12):7182-7190.
42. Torrie GM, Valleau JP. Nonphysical sampling distributions in Monte Carlo free-energy estimation: Umbrella sampling. *J Comput Phys*. 1977;23(2):187-199.
43. Hub JS, De Groot BL, Van Der Spoel D. G-whams-a free Weighted Histogram Analysis implementation including robust error and autocorrelation estimates. *J Chem Theor Comput*. 2010;6(12):3713-3720.
44. Trzesniak D, Kunz APE, Van Gunsteren WF. A comparison of methods to compute the potential of mean force. *ChemPhysChem*. 2007;8(1):162-169.
45. Khavrutskii IV, Dzubiella J, McCammon JA. Computing accurate potentials of mean force in electrolyte solutions with the generalized gradient-augmented harmonic Fourier beads method. *J Chem Phys*. 2008;128(4):044106.
46. Marrink SJ, Risselada HJ, Yefimov S, Tieleman DP, De Vries AH. The MARTINI force field: coarse grained model for biomolecular simulations. *J Phys Chem B*. 2007;111(27):7812-7824.
47. Marrink SJ, de Vries AH, Mark AE. Coarse grained model for semiquantitative lipid simulations. *J Phys Chem B*. 2004;108(2):750-760.
48. Parametrizing a new molecule. http://cgmartini.nl/index.php/tutorials-general-introduction-gmx5/parametrzining-new-molecule-gmx5; 2017. Accessed August 7, 2020.
49. Wassenaar TA, Ingólfsson HI, Böckmann RA, Tieleman DP, Marrink SJ. Computational lipidomics with insane: a versatile tool for generating custom membranes for molecular simulations. *J Chem Theor Comput*. 2015;11(5):2144-2155.
50. Kučerka N, Nieh MP, Katsaras J. Fluid phase lipid areas and bilayer thicknesses of commonly used phosphatidylcholines as a function of temperature. *Biochim Biophys Acta Biomembr*. 2011;1808(11):2761-2771.
51. Dey R, Banerjee T, Chowdhury PR, Chaudhuri S. X-ray elucidation of 17α-pregna-2,4-dien-20-yne-(2,3-d) isoxazole-17β-ol. *J Chem Crystallogr*. 2002;31(5):4-7.
52. Hanwell MD, Curtis DE, Lonie DC, Vandermeersch T, Zurek E, Hutchison GR. Avogadro: an advanced semantic chemical editor, visualization, and analysis platform. *J Cheminform*. 2012;4(1):17.
53. Liversidge GG, Cundy KC. Particle size reduction for improvement of oral bioavailability of hydrophobic drugs: I. Absolute oral bioavailability of nanocrystalline danazol in beagle dogs. *Int J Pharm*. 1995;125(1):91-97.
54. Anhalt K, Geissler S, Harms M, Weigandt M, Fricker G. Development of a new method to assess nanocrystal dissolution based on light scattering. *Pharm Res (N Y)*. 2012;29(10):2887-2901.
55. Rodrigues L, Schneider F, Zhang X, et al. Cellular uptake of self-assembled phytantriol-based hexosomes is independent of major endocytic machineries. *J Colloid Interface Sci*. 2019;553:820-833.
56. Alskär LC, Keemink J, Johannesson J, Porter CJH, Bergström CAS. Impact of drug physicochemical properties on lipolysis-triggered drug supersaturation and precipitation from lipid-based formulations. *Mol Pharm*. 2018;15(10):4733-4744.
57. Jackson MJ, Toth SJ, Kestur US, et al. Impact of polymers on the precipitation behavior of highly supersaturated aqueous danazol solutions. *Mol Pharm*. 2014;11(9):3027-3038.
58. Keemink J, Mårtensson E, Bergström CAS. Lipolysis-permeation setup for simultaneous study of digestion and absorption in vitro. *Mol Pharm*. 2019;16(3):921-930.
59. Shang L, Nienhaus K, Nienhaus GU. Engineered nanoparticles interacting with cells: size matters. *J Nanobiotechnol*. 2014;12(1):5.
60. Gupta R, Badhe Y, Mitragotri S, Rai B. Permeation of nanoparticles across the intestinal lipid membrane: dependence on shape and surface chemistry studied through molecular simulations. *Nanoscale*. 2020;12(11):6318-6333.
61. Dahan A, Beig A, Ioffe-Dahan V, Agbaria R, Miller JM. The twofold advantage of the amorphous form as an oral drug delivery practice for lipophilic compounds: increased apparent solubility and drug flux through the intestinal membrane. *AAPS J*. 2013;15(2):347-353.
62. Schittny A, Huwyler J, Puchkov M. Mechanisms of increased bioavailability through amorphous solid dispersions: a review. *Drug Deliv*. 2020;27(1):110-127.
63. Kloefer B, Hoogevest P, Moloney R, Kuentz M, Leigh MLS, Dressman J. Biorelevant media FeSSIF and FaSSIF. *Dissolution Technol*. 2010:6-13.
64. Peetla C, Stine A, Labhasetwar V. Biophysical interactions with model lipid membranes: applications in drug discovery and drug delivery. *Mol Pharm*. 2009;6(5):1264-1276.
65. Peetla C, Labhasetwar V. Effect of molecular structure of cationic surfactants on biophysical interactions of surfactant-modified nanoparticles with a model membrane and cellular uptake. *Langmuir*. 2009;25(4):2369-2377.